MOLECULAR AND CELLULAR BIOLOGY, July 1993, p. 4342–4350
0270-7306/93/074342-09$02.00/0

Vol. 13, No. 7

The Fission Yeast Ferric Reductase Gene *frp1*$^+$ Is Required for Ferric Iron Uptake and Encodes a Protein That Is Homologous to the gp91-*phox* Subunit of the Human NADPH Phagocyte Oxidoreductase

DRAGOS G. ROMAN, ANDREW DANCIS, GREGORY J. ANDERSON, AND RICHARD D. KLAUSNER*

Cell Biology and Metabolism Branch, National Institute of Child Health and Human Development, Bethesda, Maryland 20892

Received 7 December 1992/Returned for modification 11 February 1993/Accepted 2 April 1993

We have identified a cell surface ferric reductase activity in the fission yeast *Schizosaccharomyces pombe*. A mutant strain deficient in this activity was also deficient in ferric iron uptake, while ferrous iron uptake was not impaired. Therefore, reduction is a required step in cellular ferric iron acquisition. We have cloned *frp1*$^+$, the wild-type allele of the mutant gene. *frp1*$^+$ mRNA levels were repressed by iron addition to the growth medium. Fusion of 138 nucleotides of *frp1*$^+$ promoter sequences to a reporter gene, the bacterial chloramphenicol acetyltransferase gene, conferred iron-dependent regulation upon the latter when introduced into *S. pombe*. The predicted amino acid sequence of the *frp1*$^+$ gene exhibits hydrophobic regions compatible with transmembrane domains. It shows similarity to the *Saccharomyces cerevisiae FRE1* gene product and the gp91-*phox* protein, a component of the human NADPH phagocyte oxidoreductase that is deficient in X-linked chronic granulomatous disease.

Iron is an essential nutrient required for such basic cellular processes as respiration and DNA synthesis. Its unique chemistry imposes special constraints on organisms. Iron exists in two major oxidation states in aqueous media; the ferrous (Fe^{2+}) form is quite soluble, but in the presence of oxygen it oxidizes to the insoluble ferric (Fe^{3+}) form (5). Some eukaryotes, such as many plants and some fungi, resemble prokaryotes in that they secrete siderophores capable of binding ferric iron with high affinity and delivering the ferric chelate to specific receptors at the cell surface for translocation into the cytoplasm (38).

In the gut of vertebrates, the apical membrane of the enterocyte provides the interface with the environment. The absorption of iron from the diet is regulated in a manner that inversely reflects total body iron stores (4), a process that appears to be dysregulated in the common human genetic disease hereditary hemochromatosis, in which total body iron accumulation continues despite full and even excessive iron stores (37). No siderophore has been identified in the lumen of the gut, and the precise mechanism by which dietary ferric iron crosses the apical enterocyte membrane is not understood. An alternative mechanism to siderophore-mediated iron uptake which involves the extracellular reduction of ferric iron followed by the uptake of the soluble ferrous species has been postulated (27). Enzymatic ferric reduction has been described at the luminal surface of the mammalian gut (25), in endosomes of mammalian cells (20), and at the surface of iron-stressed plant roots (2). In order to directly address the possible connection between externally oriented ferric reductase activity and cellular iron uptake, we and others turned to *Saccharomyces cerevisiae* (6, 9, 17). We have recently cloned and characterized a gene from this organism required for ferric reductase activity and efficient ferric iron uptake, thus linking these two processes in an in vivo experimental system (7).

* Corresponding author.

In this study we report the molecular characterization of a ferric reductase in the fission yeast *Schizosaccharomyces pombe*. *S. pombe* and *S. cerevisiae* are as evolutionarily distant from each other as each is from vertebrates (34); thus, the evidence provided in this study that the iron uptake mechanisms that we have described in *S. cerevisiae* extend to other, evolutionarily divergent, organisms raises the possibility that vertebrates may utilize similar mechanisms for cellular iron acquisition. Comparison of the predicted sequences of the *S. pombe* and *S. cerevisiae* predicted gene products with the gp91-*phox* of the respiratory burst oxidase of human granulocytes suggests that they may constitute members of a novel family of plasma membrane electron transport proteins responsible for mobilizing cytoplasmic reducing equivalents and donating them to extracellular substrates. In the case of the *S. cerevisiae FRE1* and *S. pombe frp1*$^+$, iron may function as a substrate, whereas for the respiratory burst oxidase, the physiologic substrate is thought to be extracellular oxygen.

MATERIALS AND METHODS

Strains, growth conditions, and chemical mutagenesis. The *S. pombe* wild-type strains 972 (h^-), G-99 (h^- *ura4-294*), and G-98 (h^+ *ura4-D18 leu1-32*) (12) were used to test for the presence of iron-dependent growth and ferric reductase activity. The *S. pombe* mutant strain G-100 was derived from G-99 by chemical treatment with ethyl methanesulfonate according to standard protocols (33) and subsequent screening for a reductase-negative phenotype. The *frp1*::*ura4*$^+$ disruption/deletion strain G-101 (h^+ *leu1-32 frp1*::*ura4*$^+$) was constructed by replacing the entire chromosomal *frp1*$^+$ coding region of G-98 with a 1.8-kb *Hin*dIII fragment containing the *ura4*$^+$ gene (12). The expected disruption in the *frp1* locus of G-101 was confirmed by Southern blot analysis. Yeast strains were grown in either YEA medium or EMM defined medium (19). Iron-depleted medium was prepared by treatment of the EMM medium

with Chelex-100 resin (50 g/liter; Bio-Rad Laboratories, Richmond, Calif.) prior to addition of the 10,000× mineral mixture from which iron was omitted. The solution was sterilized by ultrafiltration. For growth on solid medium, 2% agarose was added to YEA or EMM medium. When induction of ferric reductase activity on solid EMM plates was sought, iron was omitted from the mineral mixture, but Chelex-100 treatment was not necessary. Nutrients required for growth of auxotrophic strains were added at the concentrations indicated by Sherman et al. (33). Manipulations of yeast strains such as plasmid transformation, plasmid rescue, mating, sporulation, and tetrad dissection were as previously described (19). The bacterial strain used for propagation of plasmid DNA was *Escherichia coli* DH5α (Bethesda Research Laboratories, Inc., Gaithersburg, Md.).

Plasmids. A plasmid bank including fragments of *S. pombe* genomic DNA carried on pDW238 (19), a high-copy-number plasmid with a *ura4*$^+$ marker, was a generous gift from the laboratory of Paul Nurse. Plasmid p3A1 was identified from this plasmid bank by its ability to complement the reductase-negative phenotype of strain G-100. In p3A1P, a 1.1-kb internal *Pst*I fragment has been deleted from the genomic insert of p3A1. In p3A1SH, a fragment extending between the *Hpa*I site of the insert and the *Sma*I site of the polylinker has been deleted. The pTR-138 vector was derived from the pTR vector (36) by insertion of *frp1*$^+$ sequences −138 to +217 with respect to the transcription initiation site in front of the bacterial chloramphenicol acetyltransferase (CAT) gene. pTR-114, pTR-90, pTR-66, pTR-42, and pTR-18 were derived from plasmid pTR-138 by deletion of multiples of 24 nucleotides from the 5′ end of the *frp1*$^+$ sequences. The *frp1*$^+$ sequences were amplified by polymerase chain reaction (PCR) (13) from the p3A1 plasmid, inserted into the unique *Hin*dIII and *Bam*HI sites in pTR vector, and subjected to dideoxynucleotide sequencing to confirm the fidelity of the PCR amplification and cloning steps.

Ferric reductase assay. Ferric reductase activity was measured as previously described (6, 17) with minor modifications. For the fluid phase assay, cells were collected by centrifugation at 1,000 × *g*, washed twice in distilled water, and incubated at 37°C in assay buffer (0.05 M sodium citrate [pH 6.5], 5% glucose) in the presence of 1 mM $FeCl_3$ and 1 mM bathophenanthroline disulfonate. After 30 min, cells were removed by centrifugation, and the optical density of the supernatant was measured at 520 nm. For the solid-phase assay, nylon filters (1.2-μm pore size; Biotrans ICN, Irvine, Calif.) were used to make replicas of plate-grown colonies. The replicas were incubated at 37°C for 5 min on Whatman 3MM filter paper soaked in assay buffer and then were transferred to another paper soaked in assay buffer containing 1 mM $FeCl_3$ plus bathophenanthroline disulfonate until red staining of the filter at the site of the colony was noted. This usually occurred after 5 min, but the duration of the incubation was varied in order to increase signal intensity or reduce background.

Iron uptake. Ferric iron uptake was performed as previously described (6). Cells were collected after centrifugation at 1,000 × *g*, washed twice in distilled water, and resuspended in 50 mM sodium citrate (pH 6.5)–5% glucose and incubated in 20 μM $^{55}FeCl_3$ (95 Ci/mol; Amersham Corp., Arlington Heights, Ill.). After incubation on ice at 0 or 37°C for 60 min, the cells were washed on Whatman glass microfilters under vacuum with 10 ml of 0.25 M EDTA (pH 6.5) and then with 10 ml of distilled water. The filters were dried, and emissions were measured in a scintillation counter. Ferrous uptake was determined in a similar way but in the presence of 0.1 M sodium ascorbate added to the citrate buffer.

CAT assay. Transformants were inoculated into EMM medium and grown to stationary phase. Cells were washed twice in distilled water, diluted in iron-chelated EMM medium or in EMM to which ferric iron (20 μM final concentration) was added, and grown for 8 to 14 h to induce ferric reductase activity. Cells were harvested and broken in 10 mM $MgCl_2$–20 mM Tris (pH 8)–15% glycerol in the presence of protease inhibitors (phenylmethylsulfonyl fluoride and leupeptin). Each assay analyzed 26 mg of protein for 30 min at 37°C in the presence of 0.2 mM [^{14}C] chloramphenicol (60 mCi/mmol; Dupont, NEN Research Products, Boston, Mass.) and 4 mM acetyl coenzyme A (Pharmacia LKB, Alameda, Calif.). Reaction products were extracted with ethyl acetate, lyophilized, resuspended in a minimal volume of ethyl acetate, and resolved by thin-layer chromatography for 2 h. The amount of acetylated chloramphenicol was calculated after scintillation counting.

RNA isolation, Northern (RNA) blot analysis, and primer extension. RNA was isolated, separated on formaldehyde gels, and blotted to nylon filters by previously described methods (29). The blots were probed with an α-^{32}P-labeled *frp1*$^+$ probe derived from the *Pst*I fragment of plasmid p3A1. The filters were then washed with 2× SSC (1× SSC is 0.15 M NaCl plus 0.015 M sodium citrate) and 50% formamide at 75°C and reprobed with a *S. pombe* α-tubulin probe encompassing the entire coding sequence in order to assess the quantity and integrity of RNA in each lane. Primer extension was performed according to a published protocol (1). Oligonucleotides were synthesized on a DNA synthesizer (model 381 A; Applied Biosystems, Foster City, Calif.).

Genomic DNA isolation and SSCP. *S. pombe* genomic DNA was extracted from spheroplasts by described protocols (33). Conditions for 30 cycles of PCR amplification beginning with 50 ng of genomic DNA were denaturing for 1 min at 92°C, annealing for 1 min at 55°C, and extension for 1 min at 72°C. Single-strand conformation polymorphism (SSCP) analysis was performed as previously described (20).

DNA sequencing. The DNA sequence of the p3A1 insert was determined by the method of Sanger (30), with a Sequenase kit (U.S. Biochemicals, Cleveland, Ohio). Detection of the mutated sequences identified in SSCP analysis was accomplished by subcloning the polymorphic fragments from two independent PCR amplification reactions into pEMZ3. The DNA sequence of several transformants was determined.

Nucleotide sequence accession number. The annotated nucleotide sequence has been submitted to GenBank and has been assigned accession number L07749.

RESULTS

Evidence for an externally oriented ferric reductase activity in *S. pombe*. Little is known about mechanisms of iron uptake in the fission yeast *S. pombe*, and attempts to identify siderophores have been unsuccessful (39). We tested the hypothesis that, similar to *S. cerevisiae*, *S. pombe* may express an externally directed cell surface ferric reductase involved in ferric iron uptake. The expression of a number of proteins involved in cellular iron uptake is induced by iron deprivation. These include proteins involved in the siderophore-mediated transport system of bacteria (4), transferrin receptors in mammalian cells (26), and ferric reductase in *S. cerevisiae* (6). Therefore, we searched for the presence of ferric reductase activity in intact *S. pombe* cells grown in

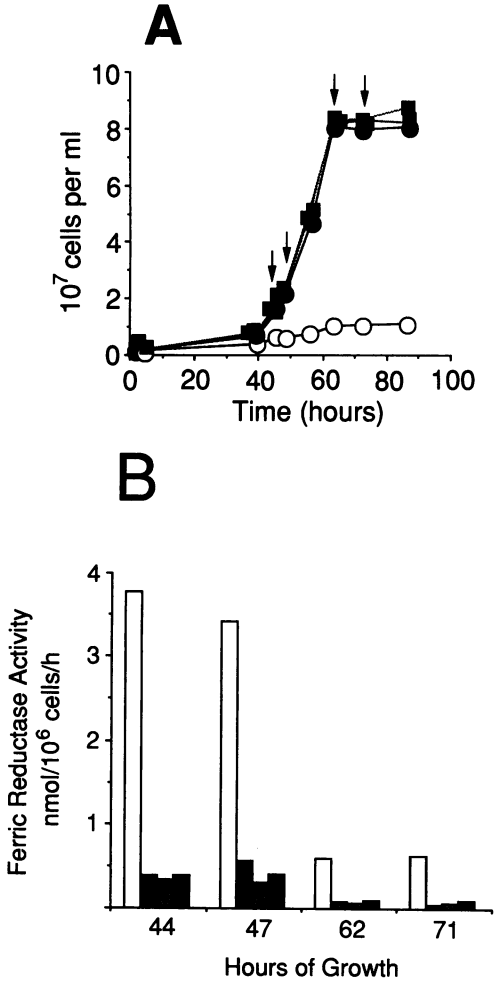

FIG. 1. Iron-dependent growth and iron-regulated ferric reductase activity in *S. pombe*. (A) *S. pombe* G-99 was grown to stationary phase in EMM minimal medium containing iron. After being washed in deionized water, the culture was diluted 1:500 into iron-chelated medium or into iron-chelated medium to which various concentrations of ferric iron were added. At the indicated times, the turbidity (optical density at 600 nm) was measured for the cultures containing 0 μM (□), 2 μM (▩), 20 μM (■), or 100 μM (■) added ferric iron. The arrows indicate times when samples were removed from the cultures (h 44, 47, 62, and 71) and analyzed for cell surface reductase activity. (B) Ferric reductase activity was measured as described in Materials and Methods at the times indicated by vertical arrows in panel A. Culture medium conditions were no added ferric iron (□) or 2 μM (▩), 20 μM (□), or 100 μM (■) added ferric iron.

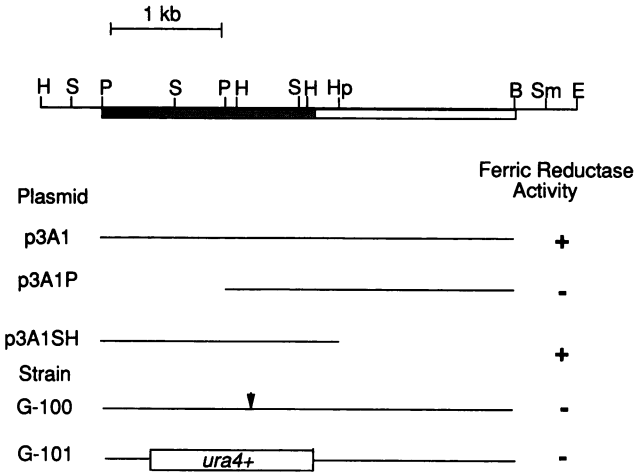

FIG. 2. Restriction map of plasmid p3A1; colocalization of the complementing activity with the *frp1*$^+$ ORF. Plasmid polylinker sequences are represented by single lines, and insert sequences are represented by bars. The stippled bar represents the *frp1*$^+$ ORF, and the blackened bar represents 5′ flanking sequences. Restriction sites are *Hin*dIII (H), *Sph*I (S), *Pst*I (P), *Hpa*I (Hp), *Bam*HI (B), *Sma*I (Sm), and *Eco*RI (E). The insert sequences contained in plasmids p3A1, p3A1P, and p3A1SH are depicted as parallel lines beneath the corresponding region of the map. The genomic sequences from strains G-100 and G-101 are similarly represented as parallel lines beneath the map. The point mutation in G-100 is indicated by the vertical arrow. Plasmids p3A1, p3A1P, and p3A1SH were introduced into the reductase-negative strain G-100, and ferric reductase activity was evaluated as shown in the column to the right side of the figure. Untransformed strains G-100 and G-101 showed negligible ferric reductase activity.

iron-depleted medium. When cells were taken from the early logarithmic or mid-logarithmic phase of growth (Fig. 1A, vertical arrows) and assayed for surface ferric reductase activity (Fig. 1B, h 44 and 47), activity was detected in the cells grown in iron-depleted medium, while in cells grown in the presence of added iron concentrations ranging between 2 and 100 μM, the activity was repressed. When cultures entered stationary phase, the activity rapidly disappeared (Fig. 1A, vertical arrows, and Fig. 1B, h 62 and 71). This repression was not prevented by iron deprivation. *S. pombe* cultures grown in iron-depleted medium exhibited reductase activity and a markedly prolonged doubling time. Under less stringent iron deprivation, reductase activity was induced, but the growth rate was unimpaired (data not shown).

An *S. pombe* mutant deficient in ferric reductase: isolation and complementation with a fragment of wild-type genomic DNA. In order to understand the role of ferric iron reduction in iron uptake in this organism, we sought to isolate a mutant deficient in ferric reductase. Haploid strain G-99 was mutagenized with ethyl methanesulfonate, and 8,000 colonies were screened for the absence of ferric reductase. One such colony was identified, and the mutant strain G-100 was derived from it. A library constructed in the pDW238 high-copy-number vector containing fragments of wild-type *S. pombe* genomic DNA was screened for the presence of sequences able to complement the reductase-deficient phenotype of the mutant strain G-100. Six thousand transformants were analyzed by filter assay for the presence of reductase activity. One such ferric reductase-positive colony was identified. The plasmid rescued from this transformant was capable of conferring the reductase-positive phenotype to the mutant G-100 upon repeat transformation, indicating that this phenotype was not due to spontaneous reversion of the original mutation but was plasmid mediated. A restriction map of the 4.3-kb insert of this plasmid (p3A1) is shown in Fig. 2.

In order to further localize the sequences of this genomic locus responsible for functional complementation, two deletions were tested. Deletion of a *Hpa*I-*Sma*I fragment from p3A1, leaving a 2-kb insert in the p3A1SH plasmid, did not affect the complementing activity. A deletion of a 1.2-kb *Pst*I fragment, generating the p3A1P plasmid, abrogated the

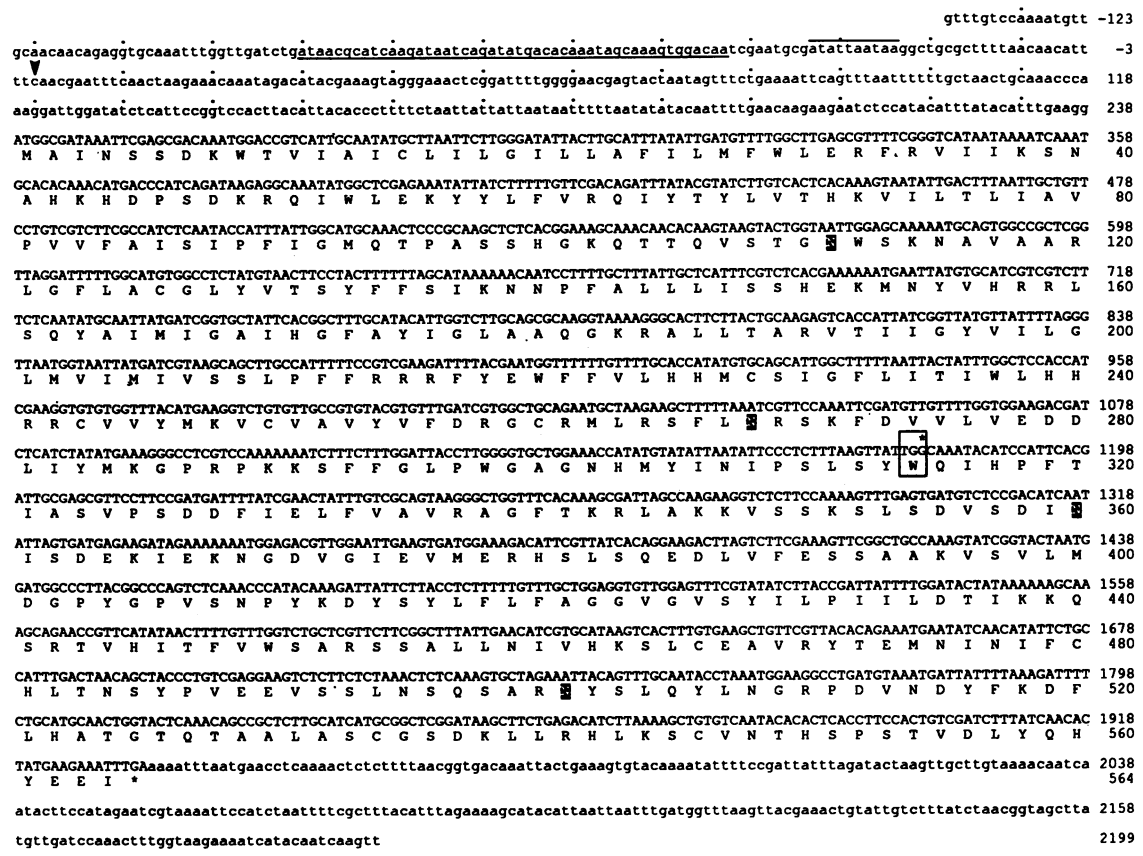

FIG. 3. Nucleotide sequence of *frp1*$^+$. Nucleotides are numbered with respect to the transcription initiation site. The C where transcription initiates is numbered +1 and is indicated by a downward arrowhead. The underlined sequences between −90 and +43 are critical for induction and iron-dependent regulation of *frp1*$^+$ transcription. A TA-rich sequence that may function like a TATA element is overlined. The predicted amino acid sequence encoded by the *frp1*$^+$ ORF is shown in one-letter code beneath each codon and numbered beginning with the initiator methionine. Potential sites for N-linked glycosylation are shown by blackening of the letter background. The G nucleotide at position 1180, which is the site of the mutation in strain G-100, is shown with an asterisk (*) over it, and the altered codon and corresponding amino acid position are boxed. Figure annotations were made with the DNADRAW (32) program.

complementing activity, indicating that this fragment contained functionally important sequences (Fig. 2).

Identification and characteristics of the complementing gene, *frp1*$^+$. The complementing region of p3A1SH includes an open reading frame (ORF) encompassing 1,692 nucleotides (Fig. 3). It encodes a predicted protein of 564 amino acids with a calculated molecular mass of 64,050 Da. There are four potential N-glycosylation sites (18) at amino acid positions 111, 268, 360, and 501 (Fig. 3). Analysis of the hydrophobicity of the protein with the Kyte-Doolittle algorithm (15) revealed several hydrophobic regions compatible with transmembrane domains. The overall pattern of the plot is compatible with a polytopic membrane protein (see below and Fig. 8). The insert contained in plasmid p3A1SH is of sufficient size to give rise to the transcript of 2 kb visualized on the Northern blot probed with a *Pst*I fragment overlapping the ORF (Fig. 2). Primer extension analysis with two distinct primers independently assigned the same transcription initiation site (+1 in Fig. 4, data not shown). This defines a region of 138 nucleotides of 5′ flanking sequence and 238 nucleotides of 5′ untranslated region preceding the ORF. A TA-rich sequence which may function like a TATA element is present between nucleotides −24 and −33 with respect to the transcription initiation site (Fig. 3). Southern blot analysis under both high- and low-stringency conditions with several restriction enzymes identified one band hybridizing with the *Pst*I probe (Fig. 2), consistent with a single gene copy per haploid genome (data not shown).

The function of this gene was further established by constructing a strain, G-101, in which the entire ORF was deleted from the haploid genome (see Materials and Methods and Fig. 2). Strain G-101 was viable but lacked measureable ferric reductase. The complementing gene was named *frp1*$^+$ since it is required for ferric reductase activity in *S. pombe*.

In order to demonstrate that the p3A1 complementing plasmid contains the wild-type allele of the mutant gene in G-100 responsible for the reductase-negative phenotype, a cross of G-101 with the mutant G-100 was performed. The diploid was sporulated, and 13 tetrads were dissected and analyzed for ferric reductase and uracil auxotrophy. In spite of a 2:2 segregation for uracil auxotrophy, all spores analyzed were scored as negative for reductase. The absence of recombination between the mutation in G-100 and the targeted deletion of the ORF of p3A1 in G-101 indicates that they are allelic.

To establish the molecular basis of the reductase-negative phenotype in strain G-100, we sought to identify the underlying mutation in the *frp1* gene. Synthetic oligonucleotides, 200 to 300 nucleotides apart, were used to PCR amplify the *frp1* gene from genomic DNA isolated from both wild-type

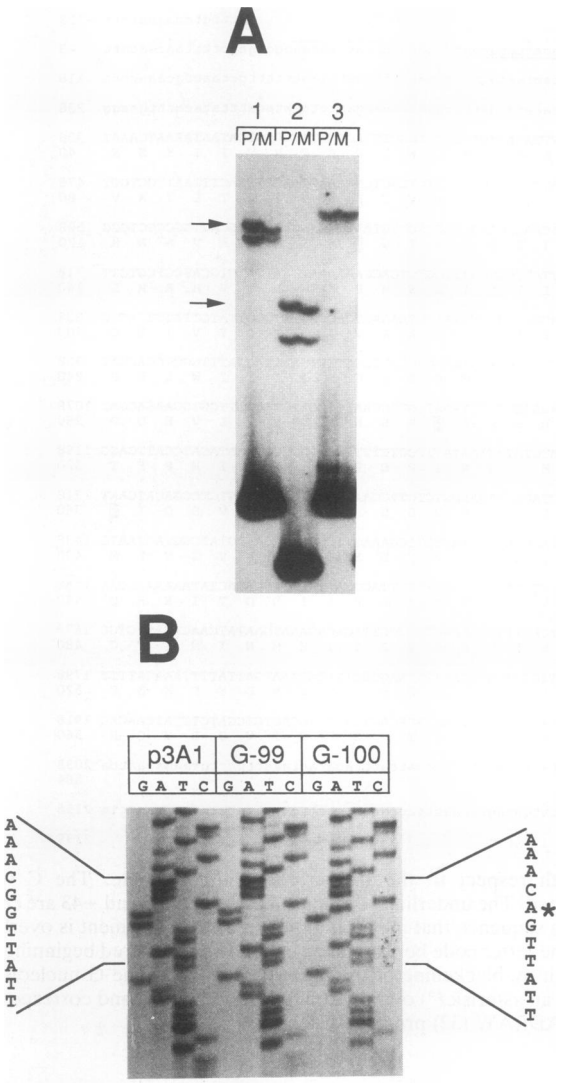

FIG. 4. Identification of the mutation in the *frp1* gene of the strain G-100 by SSCP. (A) Labeled fragments from the *frp1* genomic locus of the parental strain G-99 (P) and the mutant strain G-100 (M) were generated by PCR amplification in the presence of [α-^{32}P]dCTP. A fraction of each sample was denatured by heating and run for 14 h on a 6% polyacrylamide nondenaturing gel at 10 W. Polymorphisms were recognized as differences in the migration of the parental and mutant-amplified DNA fragments (arrows, lanes 1 and 2). Lanes 3 (P/M) show the migration of fragments exhibiting no polymorphism. (B) The amplified fragments exhibiting polymorphic migration were subcloned and subjected to DNA sequencing. From left to right are shown the sequences of the p3A1 plasmid, genomic DNA from strain G-99, and genomic DNA from the mutant strain G-100. The wild-type sequence (p3A1 and G-99) is displayed vertically on the left side, while the mutant sequence (G-100) is displayed on the right side of the figure, with an asterisk indicating the G-to-A transition.

and G-100 mutant cells. Thus, sequences covering the entire gene were amplified, including the promoter, 5′ untranslated, coding, and 3′ untranslated regions. Mutational analysis was done by using the SSCP assay as previously described (21). A single polymorphism (Fig. 4A, arrows) contained in the overlapping fragments spanning nucleotides 1258 to 1468 and nucleotides 1229 and 1380 was identified. DNA sequencing of both amplified polymorphic fragments identified a G-to-A transition in the overlapping region at nucleotide position 1180 of the *frp1*$^+$ sequence (Fig. 3 and 4B, asterisk). This resulted in the substitution of an opal stop codon (TGA) for a tryptophan codon (TGG) at codon 314 of the predicted *frp1*$^+$ ORF. If this premature stop codon is the basis for the lack of reductase activity in the G-100 strain, the *frp1* transcript should still be present. Indeed, Northern blot analysis of RNA isolated from the G-100 strain and the parental G-99 strain probed with the *frp1*$^+$ fragment confirmed the presence of a transcript of similar size in both strains (data not shown).

The *frp1* gene product is required for ferric but not ferrous iron uptake. A two-component iron uptake system utilizing a ferric reductase and a molecularly distinct ferrous transporter has been described for *S. cerevisiae* (6). Thus, in *S. cerevisiae*, ferric reductase is necessary for ferric but not for ferrous uptake. To test whether a similar system operates in *S. pombe*, we measured ferric reductase, ferric iron uptake, and ferrous iron uptake in the wild-type strain (G-99), in the *frp1-314* mutant (G-100), in the *frp1*::*ura4*$^+$ strain (G-101), and in the *frp1-314* mutant strain complemented with the cloned *frp1*$^+$ gene on a multicopy plasmid. The ferric reductase activity of these strains after induction in iron-depleted medium is depicted in Fig. 5A. As seen in Fig. 5B, ferric iron uptake was found to be deficient in both the *frp1-314* mutant strain (G-100) and in the *frp1*::*ura4*$^+$ strain (G-101). The episomal expression of *frp1*$^+$ in the mutant strain G-100 corrected both the reductase-negative phenotype (Fig. 5A), and the inability of this mutant to acquire iron when delivered in the ferric form (Fig. 5B). In contrast to the uptake of ferric iron, we found no significant differences in ferrous iron uptake among wild-type, *frp1* mutant, *frp1*::*ura4*$^+$, and complemented mutant strains. (Fig. 5C).

***frp1*$^+$ is regulated by iron at the level of transcription.** Since the ferric reductase activity of *S. pombe* is dependent on the availability of iron in the environment and the *frp1* gene product is required for ferric reduction, we examined the possibility that *frp1* gene expression might be regulated by iron availability. Wild-type *S. pombe* cultures were grown in either iron-chelated medium until reductase activity was induced or in chelated medium supplemented with ferric iron at final concentrations of 2, 20, or 100 μM (Fig. 1, h 44). RNA was extracted at this time and analyzed on a Northern blot by probing with sequences complementary to *frp1*$^+$. The probe hybridized to a mRNA of 2 kb (Fig. 6). The steady-state levels of this mRNA displayed a direction and range of regulation similar to the cell-surface reductase activity; they were induced by iron depletion and repressed by the addition of 2 μM or greater ferric iron to the growth medium (Fig. 6). The direction of the changes in *frp1* mRNA levels is compatible with the suggested function of this gene in iron uptake, i.e., expression was increased when conditions of low iron availability were encountered.

The mutant strain G-100 acquired ferric reductase activity responsive to the iron concentration of the medium when it was complemented by the *frp1* gene on the plasmid p3A1 (data not shown). To test the hypothesis that *frp1* might be regulated at the transcriptional level, a DNA fragment including 138 bp of p3A1 sequence upstream from the transcription start was linked to the CAT gene on the plasmid pTR, creating plasmid pTR-138. When this plasmid was transformed into strain G-99, CAT activity was demonstrated in iron-depleted medium, while negligible activity was observed in iron-rich medium, showing that both promoter activity and iron-dependent regulation could be trans-

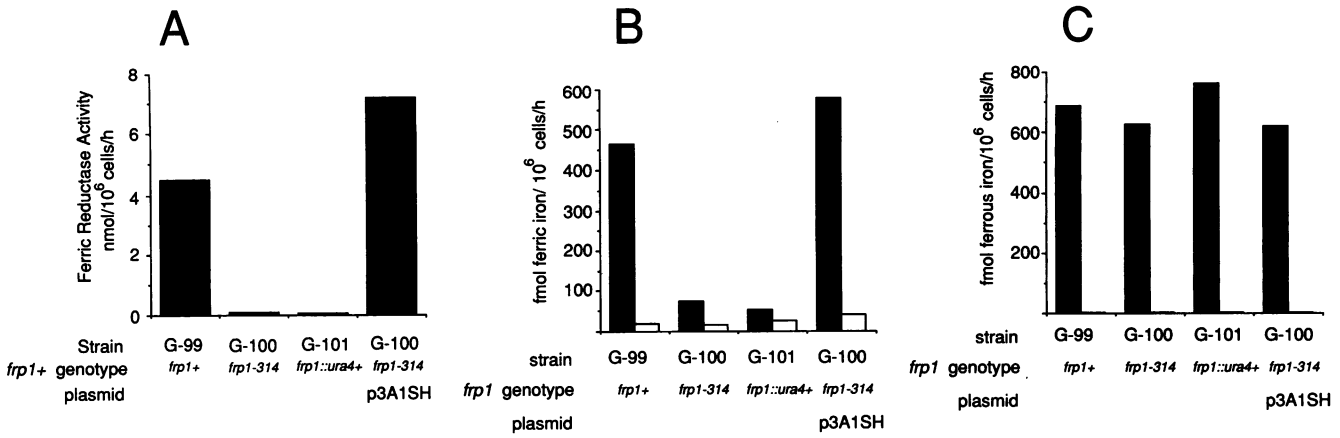

FIG. 5. Effects of *frp1*$^+$ on ferric and ferrous iron uptake. Ferric reductase-positive strain G-99 (*frp1*$^+$), mutant strain G-100 (*frp1-314*), and interruption/deletion strain G-101 (*frp1::ura4*$^+$) were grown to stationary phase in EMM medium containing iron and then transferred to iron-depleted EMM until ferric reductase activity was induced. (A) Ferric reductase activity in the above strains. (B) Ferric iron uptake in the above strains. Uptake at 37°C is shown as shaded bars and at 0°C is shown as unshaded bars. (C) Ferrous iron uptake in the same cells. Uptake at 37°C is shown as shaded bars and at 0°C is shown as unshaded bars. Each column represents an average of four separate uptake measurements (standard deviations for these measurements did not exceed 10% of the value of the measurement).

ferred to a reporter gene. The amplitude of induction of CAT activity closely followed the level of induced ferric reductase activity, suggesting that transcription initiation is a major site for *frp1*$^+$ regulation.

A more detailed analysis was performed by sequentially deleting multiples of 24 nucleotides from the 5′ end of the *frp1*$^+$ promoter sequences present in plasmid pTR-138. The constructed plasmids were initially tested for their ability to confer CAT activity under inducing conditions, i.e., in chelated medium. As shown in Fig. 7, deletion of sequences from position −138 to −91 with respect to the *frp1*$^+$ transcription initiation site had little effect on promoter activity in the absence of iron. Extending the 5′ deletion to *frp1* position −67 resulted in a partial loss of activity, and deletion to position −43 resulted in a virtually total loss of activity. When the plasmids containing the various *frp1-CAT* fusions were examined in cultures grown in the presence of iron, no effect was seen with removal of sequences between the 5′ end of the clone and position −91. Deletion to −67 resulted in the partial loss of iron-dependent repression, and deletion to −43 resulted in the loss of induced activity, so repression could not be evaluated. Thus, it seems that sequences critical for induction and iron-dependent regulation of *frp1*$^+$ transcription must lie between positions −90 and −43 with respect to transcription initiation (see under-

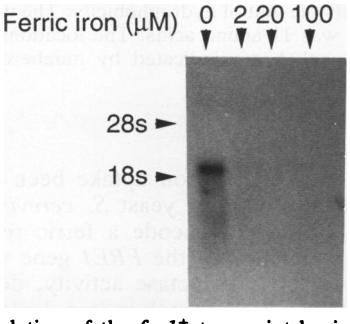

FIG. 6. Regulation of the *frp1*$^+$ transcript by iron. Total RNA was isolated from cells grown in iron-chelated medium or in the presence of 2, 20, or 100 μM added ferric iron. Ten-microgram samples were separated on a formaldehyde gel, blotted onto a nylon filter, and probed with an α-^{32}P-labeled *PstI* fragment from the *frp1*$^+$ gene. The locations of the 28S and 18S rRNA are indicated by horizontal arrows.

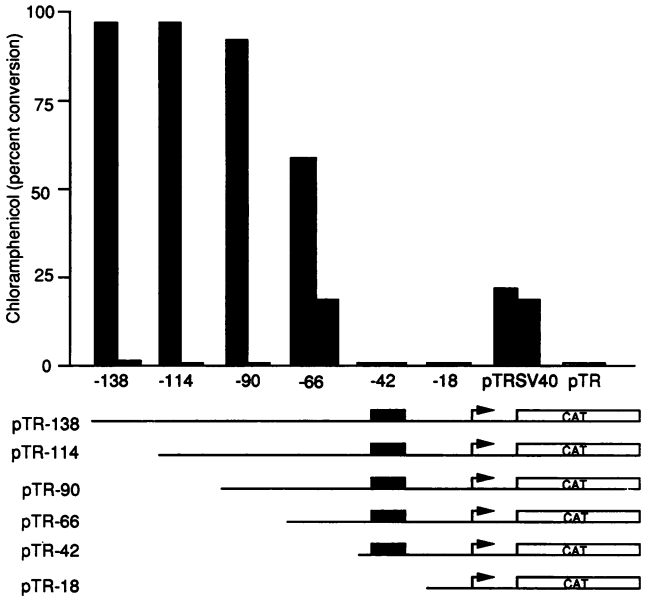

FIG. 7. Analysis of the 5′ flanking region of *frp1*$^+$. Sequences to be analyzed for promoter activity were inserted 5′ of the coding region of the bacterial reporter gene, CAT, in the plasmid pTR (36). pTRSV40 contains simian virus 40 (SV40) sequences introduced into pTR. pTR-138, pTR-114, pTR-90, pTR-66, pTR-42, and pTR-18 contain *frp1*$^+$ sequences beginning at the positions indicated by the plasmid number and ending at position +217 (see Materials and Methods). The top panel depicts data from assays of CAT activity in yeast cultures transformed with the above-mentioned plasmids and grown in the absence (shaded bars) or presence (black bars) of added iron. The plasmid inserts are diagrammed in the bottom panel, with the TATA-like element shown as a darkened box and the site and direction of transcription shown by an arrow.

lined sequence in Fig. 3). The repeated sequence TTTTTGC TCA(T/C)C implicated in the iron-dependent transcriptional regulation of the *S. cerevisiae FRE1* gene (7) was not found in *frp1*$^+$. A search of a data base containing *cis*-acting sequence elements (11) identified the motif, CAAT, which is present in inverted orientation at positions −89 to −86 and in direct orientation at positions −45 to −42 (Fig. 3). CAAT boxes constitute widely conserved sequence elements which may serve as binding sites for transcriptional activators (10). The specific role of this sequence in the *frp1*$^+$ promoter remains to be established.

Similarities among the *frp1*$^+$ gene product, the *FRE1* gene product, and the gp91-*phox* subunit of the human phagocyte NADPH oxidoreductase. Sequence comparison of the predicted *frp1*$^+$ amino acid sequence with the GenEMBL data bank (GenBank release 73.0, September 1992, and EMBL release 31.0, June 1992) by using the TFASTA algorithm (8, 23) revealed similarity only to the predicted product of *FRE1*, a gene required for ferric reductase activity in *S. cerevisiae* (7). Direct comparison of the amino acid sequences of these two predicted proteins (BESTFIT [35]) indicated 27% amino acid identity and 49% similarity with areas of more concentrated identity towards the carboxy ends. Several sequence clusters were conserved and could be aligned in the two proteins (Fig. 8). The FRE1 predicted protein bears sequence similarity to gp91-*phox*, a membrane component of an oxidoreductase present in human granulocytes (22). Therefore, we compared the *frp1* gene product with gp91-*phox*. The level of amino acid identity, 20%, and similarity, 48%, is of borderline statistical significance, but several clustered amino acid identities and similarities seen in the Frp1/FRE1 predicted protein alignment were also present in gp91-*phox* (Fig. 8). In particular, the amino acid sequence HPFTXXS (motif 2, Fig. 8), which has been proposed to function in flavin adenine dinucleotide (FAD) binding in the respiratory burst oxidase (31), is well conserved in the two yeast sequences. Two other sequences, proposed to represent peptide loops involved in NADPH binding, the glycine-rich motif (motif 4, Fig. 8) as well as the cystine-glycine couplet (motif 5, Fig. 8) (31) are also conserved.

Examination of the Kyte-Doolittle hydropathy profile of the Frp1 predicted protein reveals multiple hydrophobic regions that are consistent with transmembrane domains. Moreover, if the hydropathy profiles of the three proteins, Frp1, FRE1, and gp91-*phox*, are aligned (Fig. 8B), the similarities can be appreciated. FRE1 begins with a sequence compatible with a membrane insertion leader peptide (7) followed by a hydrophilic amino-terminal region not found in the other two proteins. Beyond this region of FRE1, all three predicted proteins manifest multiple hydrophobic domains followed by an approximately 300-amino-acid hydrophilic carboxy terminus. Each protein has a hydrophobic domain within this carboxy-terminal region in which motif 4 is found. Furthermore, all five of the conserved motifs are located in this carboxy-terminal region, and they are located at similar positions when the three proteins are aligned (Fig. 8B).

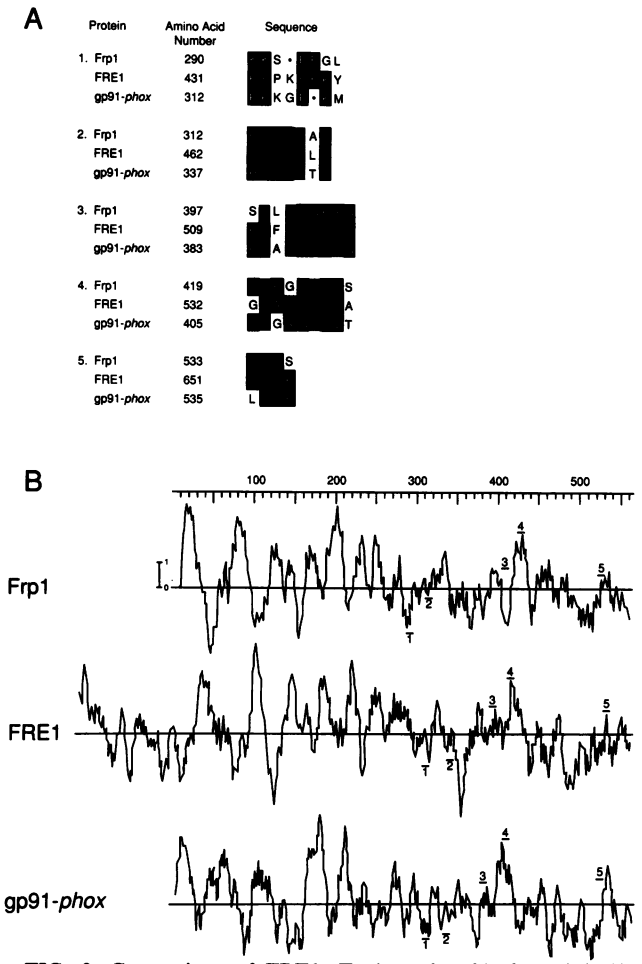

FIG. 8. Comparison of FRE1, Frp1, and gp91-*phox*. (A) The amino acid sequences of the predicted proteins were aligned to each other pairwise by using the BESTFIT algorithm (35). Clustered amino acid identities conserved among the three sequences were identified by examination of the pairwise alignments by eye. The column labeled Amino Acid Number indicates the first amino acid in the sequence motif. The letters with blackened background represent amino acids which are identical among the sequences being compared. Shaded residues indicate conservative changes among the aligned sequences. (B) The Kyte-Doolittle hydrophobicity plots of Frp1, FRE1, and gp91-*phox* were aligned at the carboxy-terminal end. The numbers on the horizontal axis correspond to amino acid residues of the Frp1 predicted protein sequence (Fig. 4). The vertical bar depicts the unit of hydrophobicity. The window size for this examination was 11 amino acids. The locations of the amino acid motifs in panel A are indicated by numbered bars in the hydrophobicity plots.

DISCUSSION

The mechanisms by which iron crosses membranes to enter eukaryotic cells are yet to be fully understood. While a role for enzymatic ferric reduction at the cell surface has been long proposed (2, 3, 17, 27), only recently has the molecular characterization of such a reductase and proof of its involvement in cellular iron uptake been provided. In those studies in the budding yeast *S. cerevisiae*, a gene, *FRE1*, which is likely to encode a ferric reductase was identified (6, 7). Deletion of the *FRE1* gene was found to result in reduced ferric reductase activity, deficient ferric iron uptake, and impaired growth in iron-depleted medium. Whether this system was limited to *S. cerevisiae* or representative of a more generalized process preserved in other eukaryotic organisms was not known. For this reason we undertook an analogous study with *S. pombe* to molecularly characterize a possible ferric reductase gene (*frp1*$^+$). This gene is required for both ferric reduction and ferric iron

uptake. We show that not only does it share multiple structural and functional features with the *S. cerevisiae FRE1* gene, but it also preserves a similar mechanism of regulation.

Several lines of evidence support the idea that the *frp1*$^+$ gene of *S. pombe* encodes a ferric reductase. (i) *frp1*$^+$, when carried on a plasmid, was capable of full complementation of the chromosomal mutation in a strain lacking ferric reductase activity (G-100). (ii) A haploid strain (G-101) carrying an interruption/deletion at the chromosomal *frp1* locus was deficient in ferric reductase activity. (iii) The point mutation responsible for the ferric reductase deficiency in G-100 did not recombine with the deleted *frp1* locus in G-101, indicating that they are allelic. (iv) The abundance of the *frp1*$^+$ transcript was regulated by iron availability in the growth medium.

Although it is still formally possible that the *frp1*$^+$ gene encodes a positive regulator of the ferric reductase, the gene product more likely represents a structural component of the reductase itself. This is supported by the homology with the FRE1 gene product of *S. cerevisiae*, thought to be a structural component of the ferric reductase, and with the gp91-*phox* component of the human respiratory burst oxidase. The latter is a plasma membrane component of a well-characterized oxidoreductase present in phagocytic cells, capable of transferring electrons from cytoplasmic NADPH to molecular O_2, generating microbicidal O_2^- (22). When the predicted protein sequences of Frp1, FRE1, and gp91-*phox* are aligned, a striking resemblance is seen in their hydropathy profiles. A number of strongly hydrophobic regions suggesting multiple transmembrane domains are clustered in the amino-terminal portion of each protein. The carboxy-terminal 300 amino acids are generally hydrophilic, with the exception of one aligned hydrophobic stretch in each. Within this region, five conserved motifs are well aligned in the three proteins. One of these, motif 2 of Fig. 8 (HPFTXXS), was recently identified as a possible FAD binding site for gp91-*phox* (31). The basis for this proposal is the limited amino acid sequence similarity with the crystallographically demonstrated FAD binding site of the spinach ferredoxin $NADP^+$ reductase (14). The similarity of the spinach protein sequence (RLYSIAS) with motif 2 (HPFTXXS), however, is limited, whereas motif 2 is conserved in each of the yeast sequences.

Although for the respiratory burst oxidase the precise path of electrons from cytoplasm to extracellular substrate has not been defined, it is thought that movement of electrons may occur from cytoplasmic NADPH to FAD to heme and then to extracellular oxygen (31). Heme, like FAD, is an essential cofactor for this process. gp91-*phox* is thought to participate in heme binding, although the protein domains interacting with the heme have not been identified (24). In this regard, it is interesting to note that heme-deficient yeast strains appear to lack ferric reductase activity (16). The yeast Frp1 and FRE1 gene products of *S. pombe* and *S. cerevisiae*, respectively, may resemble gp91-*phox* in participating in the transport of electrons from cytoplasm to an extracellular substrate via FAD and heme intermediates. In the case of the two yeast proteins, the substrate is (but may not be limited to) ferric iron, while for gp91-*phox*, the substrate is dioxygen. These three proteins may constitute a distinct family of flavocytochromes capable of moving electrons across the plasma membrane (31).

In spite of the many similarities between the *frp1*$^+$ and *FRE1* genes, the degree of amino acid identity between the *S. pombe* Frp1 and the *S. cerevisiae* FRE1 predicted gene products is quite limited. Additionally, despite the fact that the expression of both of these genes is transcriptionally regulated in response to iron, the promoters lack obvious common consensus sequences. Thus, the data presented here suggest that in comparing the iron uptake systems of *S. cerevisiae* and *S. pombe*, there are basic similarities of structure and regulation but limited sequence conservation. While similar iron uptake mechanisms are likely to operate in vertebrates, as in these two divergent yeasts, these studies suggest that the responsible proteins may function with little overall sequence conservation.

REFERENCES

1. **Caroline, D., M. Favreau, P. Dunsmuir, and J. Bedbrook.** 1987. Confirmation of the relative expression levels of the petunia (Mitchell) rbcS genes. Nucleic Acids Res. **15**:4655–4668.
2. **Chaney, R. L., J. C. Brown, and L. O. Tiffin.** 1972. Obligatory reduction of ferric chelates in iron uptake by soybeans. Plant Physiol. **50**:208–213.
3. **Crane, F., H. Roberts, A. W. Linnane, and H. Low.** 1982. Transmembrane ferricyanide reduction by cells of the yeast *Saccharomyces cerevisiae*. **14**:191–205.
4. **Crichton, R. R.** 1991. Solution chemistry of iron in biological media, p. 13–28. *In* R. R. Crichton, Inorganic biochemistry of iron metabolism. Ellis Horwood Limited, West Sussex, England.
5. **Crichton, R. R., and M. Charloteaux-Wauters.** 1987. Iron transport and storage. Eur. J. Biochem. **164**:485–506.
6. **Dancis, A., R. D. Klausner, A. G. Hinnebusch, and J. G. Barriocanal.** 1990. Genetic evidence that ferric reductase is required for iron uptake in *Saccharomyces cerevesiae*. Mol. Cell. Biol. **10**:2294–2301.
7. **Dancis, A., D. G. Roman, G. J. Anderson, A. G. Hinnebusch, and R. D. Klausner.** 1992. Ferric reductase of Saccharomyces cerevisiae: molecular characterization, role in iron uptake, and transcriptional control by iron. Proc. Natl. Acad. Sci. USA **89**:3869–3873.
8. **Devereux, J., P. Haeberli, and O. Smithies.** 1984. A comprehensive set of sequence analysis programs for the VAX. Nucleic Acids Res. **12**:387–395.
9. **Eide, D., S. Davis-Kaplan, I. Jordan, D. Sipe, and J. Kaplan.** 1992. Regulation of iron uptake in *Saccharomyces cerevisiae*. J. Biol. Chem. **267**:20774–20781.
10. **Forsburg, S. L., and L. Guarente.** 1989. Identification and characterization of HAP4: a third component of the CCAAT-bound HAP2/HAP3 heteromer. Genes Dev. **3**:1166–1178.
11. **Ghosh, D.** 1992. TFD: the transcription factors database. Nucleic Acids Res. **20**(Suppl):2091–2093.
12. **Grimm, C., J. Kohli, J. Murray, and K. Maundrell.** 1988. Genetic engineering of Schizosaccharomyces pombe: a system for gene disruption and replacement using the Ura4 gene as a selectable marker. Mol. Gen. Genet. **215**:81–86.
13. **Innis, M. A., and D. H. Gelfand.** 1990. Optimization of PCRs, p. 3–12. *In* M. A. Innis, D. H. Gelfand, J. J. Sninsky, and T. J. White (ed.), PCR protocols. Academic Press, Inc., San Diego, Calif.
14. **Karplus, P. A., M. J. Daniels, and J. R. Herriott.** 1991. Atomic structure of ferredoxin-$NADP^+$ reductase: prototype for a structurally novel flavoenzyme family. Science **251**:60–66.
15. **Kyte, J., and R. F. Doolittle.** 1982. A simple method for displaying the hydrophobic character of a protein. J. Mol. Biol. **157**:105–132.
16. **Lesuisse, E., and P. Labbe.** 1989. Reductive and non-reductive mechanisms of iron assimilation by the yeast Saccharomyces cerevesiae. J. Gen. Microbiol. **135**:257–263.
17. **Lesuisse, E., F. Raguzzi, and R. R. Crichton.** 1987. Iron uptake by the yeast Saccharomyces cerevisiae: involvement of a reduction step. J. Gen. Microbiol. **133**:3229–3236.
18. **Marshall, R. D.** 1972. Glycoproteins. Annu. Rev. Biochem. **41**:673–702.
19. **Moreno, S., A. Klar, and P. Nurse.** 1991. Molecular genetic analysis of fission yeast Schizosaccharomyces pombe, p. 795–

823. *In* C. Guthrie and G. R. Fink (ed.), Guide to yeast genetics and molecular biology. Academic Press, Inc., San Diego, Calif.
20. **Nunez, M.-T., V. Gaete, J. A. Watkins, and J. Glass.** 1990. Mobilization of iron from endocytic vesicles. J. Biol. Chem. **265**:6688–6692.
21. **Orita, M., T. Suzuki, T. Sekiya, and K. Hayashi.** 1989. Rapid and sensitive detection of point mutations and DNA polymorphisms using the polymerase chain reaction. Genomics **5**:874–879.
22. **Orkin, S. H.** 1989. Molecular genetics of chronic granulomatous disease. Annu. Rev. Immunol. **7**:277–307.
23. **Pearson, W. R., and D. J. Lipman.** 1988. Improved tools for biological sequence comparison. Proc. Natl. Acad. Sci. USA **85**:2444–2448.
24. **Quinn, M. T., M. L. Mullen, and A. J. Jesaitis.** 1992. Human neutrophil cytochrome b contains multiple hemes. J. Biol. Chem. **267**:7303–7309.
25. **Raja, K. B., R. J. Simpson, and T. J. Peters.** 1992. Investigation of a role for reduction in ferric iron uptake by mouse duodenum. Biochem. Biophys. Acta **1135**:141–146.
26. **Rao, K. K., D. Shapiro, E. Mattia, K. Bridges, and R. D. Klausner.** 1985. Effects of alterations in cellular iron on biosynthesis of transferrin receptor in K562 cells. Mol. Cell. Biol. **5**:595–600.
27. **Romheld, V.** 1987. Existence of two different strategies for the acquisition of iron in higher plants, p. 353–374. *In* G. Winkelmann, D. van der Helm, and J. B. Neilands (ed.), Iron transport in microbes, plants and animals. VCH Verlagsgesellschaft, Weinheim, Germany.
28. **Russell, P.** 1989. Gene cloning and expression, p. 243–271. *In* A. Nasim, P. Young, and B. F. Johnson (ed.), Molecular biology of the fission yeast. Academic Press, Inc., San Diego, Calif.
29. **Sambrook, J., E. F. Fritsch, and T. Maniatis.** 1989. Molecular cloning: a laboratory manual, 2nd ed. Cold Spring Harbor Laboratory, Cold Spring Harbor, N.Y.
30. **Sanger, F., S. Nicklen, and A. R. Coulson.** 1977. DNA sequencing with chain-terminating inhibitors. Proc. Natl. Acad. Sci. USA **74**:5463–5467.
31. **Segal, A. W., I. West, F. Wienjes, J. Nugent, A. J. Chavan, B. Haley, R. C. Garcia, H. Rosen, and G. Scrace.** 1992. Cytochrome b-245 is a flavocytochrome containing FAD and the NADPH binding site of the microbicidal oxidase of phagocytes. Biochem. J. **284**:781–788.
32. **Shapiro, M.** 1990. DNAdraw—a program for drawing DNA sequences. Binary **2**:187–190.
33. **Sherman, F., G. R. Fink, and J. B. Hicks.** 1989. Laboratory course manual for methods in yeast genetics. Cold Spring Harbor Laboratory, Cold Spring Harbor, N.Y.
34. **Sipiczki, M.** 1989. Taxonomy and phylogenesis, p. 431–452. *In* A. Nasim, P. Young, and B. F. Johnson (ed.), Molecular biology of the fission yeast. Academic Press, Inc., San Diego, Calif.
35. **Smith, T. F., and M. S. Waterman.** 1981. Comparison of biosequences. Adv. Appl. Math. **2**:482–489.
36. **Toyama, R., and H. Okayama.** 1990. Human chorionic gonadotropin a and human cytomegalovirus promoters are extremely active in the fission yeast Schizosaccharomyces pombe. FEBS Lett. **268**:217–221.
37. **Walters, G. O., A. Jacobs, M. Worwood, D. Trevett, and W. Thomson.** 1975. Iron absorption in normal subjects and patients with idiopathic haemochromatosis: relationship with serum ferritin concentration. Gut **16**:188–192.
38. **Winkelmann, G., and H. Huschka.** 1987. Molecular recognition and transport of siderophores in fungi, p. 317–336. *In* G. Winkelmann, D. Van der Helm, and J. B. Neilands (ed.), Iron transport in microbes, plants and animals. VCH Publishers, Inc., New York.
39. **Winkelmann, G., J. B. Nielands, K. Krystyna, B. Schwyn, M. Coy, R. T. Francis, B. H. Paw, and A. Bagg.** 1987. Comparative biochemistry of microbial iron assimilation, p. 3–13. *In* G. Winkelmann, D. Van der Helm, and J. B. Neilands (ed.), Iron transport in microbes, plants and animals. VCH Publishers, Inc., New York.